How the central domain of dystrophin acts to bridge F-actin to sarcolemmal lipids

Article *in* Journal of Structural Biology · November 2019

DOI: 10.1016/j.jsb.2019.107411

CITATIONS
0

READS
53

14 authors, including:

Angélique Cheron
Université de Rennes 1
47 PUBLICATIONS **1,042** CITATIONS
SEE PROFILE

Thomas Chenuel
Sorbonne Université
2 PUBLICATIONS **2** CITATIONS
SEE PROFILE

Marie-Sousai Appavou
Forschungszentrum Jülich
109 PUBLICATIONS **1,023** CITATIONS
SEE PROFILE

Anne Martel
Institut Laue-Langevin
103 PUBLICATIONS **867** CITATIONS
SEE PROFILE


Check for updates

(DGC) wi
1991; Ibraghimov-B
the dystrophin protein are locat
central domain is also thought to play a key
membrane cytoskeleton and the extracellular
central domain of dystrophin comprises 24 spec
proximately 100 residues each in which some s
been shown to interact with numerous partners
oxide synthase (nNOS) (Lai et al., 2009), F-ac
1999) and lipids (DeWolf et al., 1997; Leg
central domain was previously described as
in silico (Legrand et al., 2011) and *in vitr*
analyses showed that the central domain ca
a straight and passive linker between ABD
its filamentous structure is believed to ha
role in the scaffolding of muscle cells t
cytoskeleton (Amann et al., 1998; Sarki
lipids (Zhao et al., 2016).

Mutations in dystrophin are the ca
disease, Duchenne muscular dystroph
progressive form of muscular dystrop
disorder affecting 1:5000 boys (Stark
destabilizes muscle membranes. Int
the dystrophin gene (*DMD*) that
termini of the protein but elimina
cause the milder Becker muscular
et al., 2015). As observed in
therefore can tolerate interna
central domain and the amino-
protein resulting in a more o
severity of the disease is not
but much more to sophisti
patterns of the shortened d
2015). Therapeutic strate
possible by skipping or
expression of truncated
2012). In parallel, due
tors, transport and exp
called mini- or microd
(Belanto et al., 2014
cise consequences o
dystrophin are not
lack of knowledg
interactions. Giv
shortened dystr
properties com
however rem
type dystrop
standing at
actin and
analyze t
dystroph

Bin
phin.
now
(Sin
cr
a

nown on Fig.

according to the align-

R1-3	*GS* EVNLD…QISQ		
R11-15	*GS* FQKPA…LNFAQ		
R8-15	(HIS_6tev*)* RKEAL…LNFAQ	100.2	861
R11-19	(HIS_6tevthb) FQKPA… LLQEL	116.8	997
ABD1	*GS* LWWEE…IQEVE	29.1	253

Residues in italics are residual residues from a
Human dystrophin (Uniprot P11532).

2.2. DYS R1-3 cloning and expression in E. co

The R1-3 fragment was produced and
scribed (Dos Santos Morais et al., 2018).

2.3. DYS R11-15 cloning and expression i

The DYS R11-15 (F_{1461}-Q_{1973}) fragm
pTG11025 plasmid DNA with the Dp
Transgene SA, Strasbourg France) wi
NdeI or XhoI restriction cassette (In
also including a 6xHis tag sequence
site in the N-terminal region. PCR p
DNA polymerase (NEB), dig
NucleoSpin kit) and inserted into
XhoI restriction sites. The His-t
duced in *E. coli* BL21(DE3) strai
37 °C and purified by immob
(IMAC) on Ni-Sepharose colun
the manufacturer instruction
cleavage and the proteins w
chromatography column (H
Healthcare) equilibrated w
and 0.1 mM EDTA, pH 7
stained with Coomassie
trophotometrically usin
280 nm of 45,950 M^{-1}

2.4. DYS R8-15 and

Extended (8 ex
fragments were a
ment was inserte
into pFastBacH
serted at the Ba
including a th
were verifie
transferred
bacmid D
bacmid D
structio
for up

Re rcular
culo rimeter
tem ed in the
pH . The per-
(ux value of
e ellipticity at
nce of a coiled-
or R11-15-bicelle
m 200 to 240 nm in
corresponding to the
respective spectra. The
l lipid concentration was

Bicelles were
phospho-L-serine-N-(7-nitro-2–1,
centration of 15 mM of lipids (~50 μM of bicel
and the [DMPC]/[DMPS] (mol/mol) ratio into
maintained equal to 2 (see Dos Santos Morais
information). The bicelles were titrated with a
of R11-15 from 184 to 165 to 2.5–2.2 μM. The
loaded into Monolith NT premium capilla
thermophoresis was measured with a Mon
(NanoTemper). Instrument parameters were
power, 40–60% MST power, and 5/20/5
surement temperature was 22 °C or 26 °C
Data were analyzed with the NT MO Affi
(NanoTemper).

2.10. Actin polymerization and sedimenta

Globular actin (G-actin) was prep
scribed previously (Winder et al., 199
performed as described in (Sarkis et
actin stored in G buffer (2 mM Tris
thiothreitol, 0.2 mM $CaCl_2$ and 1
merization buffer (F buffer; final c
150 mM NaCl, 2 mM ATP, 50 mM
threitol) and allowed the polyme
Actin polymerization was asses
sedimentation assays, 50–100-
ultracentrifuge tubes. The fina
0–150 μM for DYS R11-15.
were centrifuged for 30 min
pellets were analyzed by SD
blue and the amounts of p

*2.11. Click-chemistry, che
coupled with mass spectro*

2.11.1. R11-15 – F-act

F-actin and R11-1
polymerisation buffe
((1-ethyl-3-(3-dime
Thermofisher scie
60 min at 20 °C.
stained by Coom
monomer-one
small pieces.

2.11.2. R11-

HZB an
(3-pent-4-
line (pac
diazirine
(Haber
R11-1
prot
diat
SD
(

ne
mn
flow-
elution
A 1 mM,
1 mM, gly-
continuously
time between
buffer scattering
buffer scattering
curves displaying a
re averaged and were
to absolute unit, frame
ith FOXTROT. Data were
015).

R11-1

2.12.2. SAXS data analysis

Analyses were performed as described in De
Briefly, all data processing and analysis were
Scatter software (http://www.bioisis.net/), and
ATSAS suite (Franke et al., 2017). The distance
(r) and the maximum particle diameter (DMAX
the GNOM program. The overall ab initio mo
ment R11-15 were obtained from the SAXS ex
in Delalande *et al*. Ab initio models for other f
19) where obtained using the GASBOR pro
the scattering profiles were fitted to a q_{max}
Following a similar protocol to the one
hundred independent GASBOR computati
scattering profile, to factor the decrease
sociated with the increased fragment siz
best GASBOR computations, with the s
converted to volume grid constraints
interactive flexible fitting simulations
(Molza et al., 2014). Before simulati
molecular shape were aligned along
then rotated 10 times around the l
180° head-to-tail rotation to excha
performing 10 more rotations. Th
tions, 2 directions) were adjust
refined by standard energy mini
models were selected upon ev
obtained using PROCHECK (La
and Sander, 1983; Touw et al.
their theoretical SAXS curves
2017).

2.12.3. Small-angle neutro

Preparatory work w
Garching), and PACE (L
tions were done on D
sample-to-detector dis
4.7 to 7 Å ($\Delta\lambda/\lambda \sim 10$
the largest one, wh
wavelength, and *2*
performed in 1 m
tained are in abs
buffer at 22 °C. P
rehydration was
perfect buffer
by three suc
MWCO 10 k
Healthcare)
lipid conc
Valentini

R11-
R11
R1

2.12

s

ns ABD2
~ 1.9 (Fig.
ero-distance
t analyzed by
ain 1) fragments
trols respectively.
expected size of one
rent MW of ~100 kDa
served in the absence of
EDC, a 130–140 kDa band
ow in Fig. 1A and B and Fig.

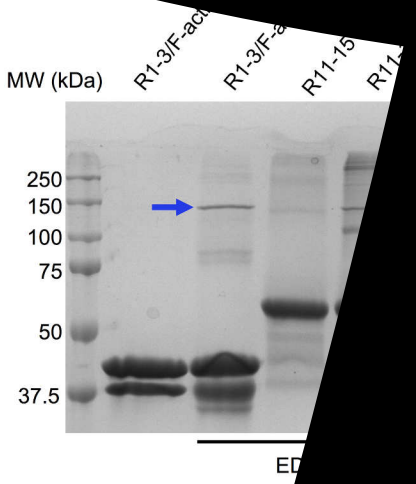

Fig. 1. (A) SDS-PAGE analysis of EDC ind
final concentrations of 5 μM were incub
digested and analysed by MS. Blue arro
size of one monomer of R11-15 (ABD2)
binding domain 1) displayed as a posi
were centrifugated at 100.000 g. Pell
were excised, trypsin digested and a
ABD1 EDC-covalently cross-linked t

S1C). In the R1-3F-actin EDC m
present at 130–140 kDa, a ba
multimer and no cross-linked
fied. ABD1 used as a positiv
actin in a ~70 kDa heterodi
in Tables S1 and Appendix

From the 100 kDa ED
the trypsin proteolysis p
from actin that are foun
are shown in Table S1
lated by MS with a h
or Val98 and Lys11
close contact with
(Fig. S1A). Corres
dystrophin ABD2
interaction with
R12 or R15. T
Ser1517 to Ar
repeat R11,
Arg1930 in

3.1.2. Li
organiza

We
memb
viou
bic
m
(

UV
cFA
arent
of the
d(s) were
zed by MS.
esponding to
however, one
fatty acid in the
obtained for the
tion is presented in
peptide ($_{1667}$AEE…
C in repeat R12 of the

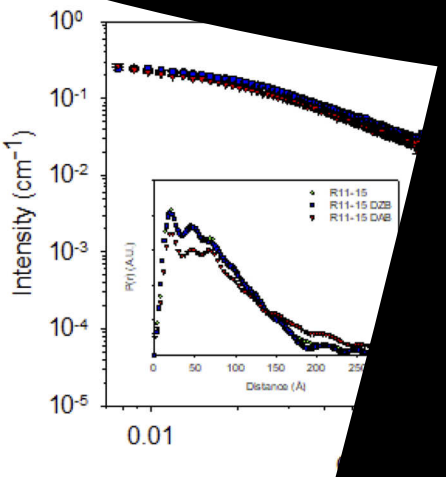

Fig. 2. (A) SANS scattering curves of dystr
(red). Inset: (left) Pair-distribution functi
interaction with anionic bicelles and (r
discrepancy (NSD) are shown, surround
zwitterionic-pacFA or anionic-pacFA bi
into small pieces and analyzed by MS

3.1.3. Dystrophin ABD2 interacts
lipids simultaneously

Ternary complexes compr
were studied *in vitro*. Only an
periments, due to the nature
sarcolemma (Fiehn et al.,
(Legarnier et al., 2009; S
ABD2/F-actin complex w
anionic bicelles containi
duced cross-linking was
the samples is shown o

Four bands inclu
(~130 kDa) and CL3
shown in Table S1 (
cross-peptides were
smear band. Inter
experiment preser
between actin a
($_{1667}$AEEWLNLI
are summarize
associated wi
exclusively i
repeat 12 c
complex, f

Actin
and R15
precise
in rep
actin
pep
ac
a
f

st
tact
con-
act fre-
ears that
with sub-
hest contact
32 interacting
, the two most
observations are
obtained from XL-
the calculations, the
ng the theoretical com-
D2–F-actin mapping ex-

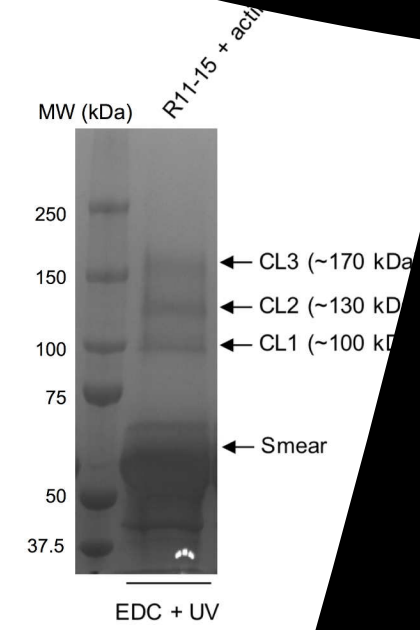

Fig. 3. (A) SDS-PAGE analysis
incubated in the presence of ani
corresponding to one monome
not detectable by SDS-PAGE)
by mass spectrometry. (B) Pe
fragment (grey); (C) 3D m
contact ABD2 (blue) mapp

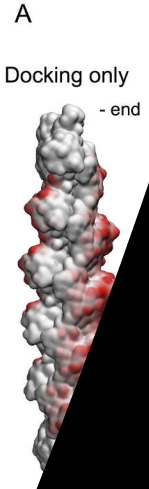

st
on-
ction
ft), as
ordance
l interac-
and F-actin

that enables the
tection as the main
peat R12 due to its
disengagement of the
with the actin filament
linker. On the contrary,

ized at th
role in accommoda
appeared at this stage that none o
contact from both repeats R11 and R15 in the sa
as we can hypothetize from co-sedimentation a
measurements found in the literature (Aman
Rybakova et al., 2002). Nevertheless, these do
vided high quality orientations for each isola
repeats towards F-actin. They were then f
structures for final improvements incorporati

3.2.3. The ABD2 model could contact two di
microfilament

Interactive flexible docking is a tech
models as we already discussed earlier (
interactive simulations, we explored the
positioning of repeats R11 and R15 relati
of distance (number of actin units separ
from + 1 to + 6) and topology (same
To achieve this, we fixed either the p
R15 according to the best models o
ciple shown in Fig. 5A).

All the best models computed
same type of simulations, namely
restrained and the rest of the dystr
the contacts experimentally mapp
closely characterizing the main
involved in the interaction betw
electrostatics should play a ke
ever, the edge of the actin
dystrophin could also be cr
through specific hydrophob
ison of contact analysis
mapping, we can conclu
ideally located on oppos
bearing the best evaluat
contact analysis with
subunits along the F
assays have a stoichi

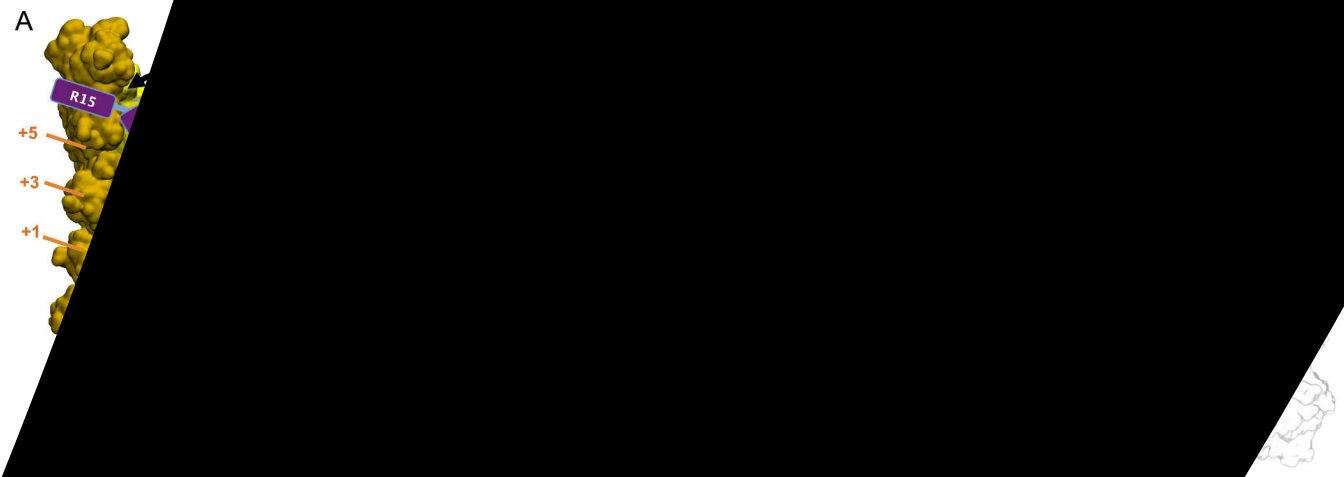

F
by the previous
n repeat R15. The
ects on the structure
volume) and verifying
volume for F-actin and
ng surfaces between both
(D) Molecular Hydrophobic
o +1 (yellow, hydrophobic).

repeat
R15-16 mini-hinge.
could suffer from these missing
R11-19 dystrophin fragments and analyzed the
angle X-ray scattering approach combined wit
fitting techniques (Molza et al., 2014). Both fra
in insect cells, and purity was assessed by SD
spectra show that both proteins exhibit a ty
structure (Fig. S6B) and SAXS curves typical of
with elongated shapes were obtained (Fig.
measured indicate that the radius of gyration
90 Å for R11-19 (Fig. S6D). Thus the dystrop
elongated in solution than the R8-15 fragm
one additional repeat. This feature is well il
models generated for each of the fragm
quality $\chi 2$ values of their related theoreti
R8-15 and 0.8 to 0.9 for R11-19) and th
initio models (NSD < 3.4 Å for R8-15
support the relevance of using these
flexible fitting. The SAXS-based atomi
new central domain fragments (S
SASBDB), were finally used to prod
complex with F-actin, dystrophin
maximizing the overlapping regio
ments (R8-15 and R11-19) and th
9, R11-15 and R16-19) (Delaland
subdomain model in good agree
at the linker regions (Fig. S7A a
SAXS-based model according t
was achieved without structu

4. Discussion

4.1. Dystrophin ABD2 is de
repeat R11 and repeat R1

Until now, the bou
domain were still und
acting region ranging
1996; Amann et al.,
was sufficient for t
actin (Sarkis et a
stability, we chos
the presence of
(and a small ne
R15. On the ac
3 to be the

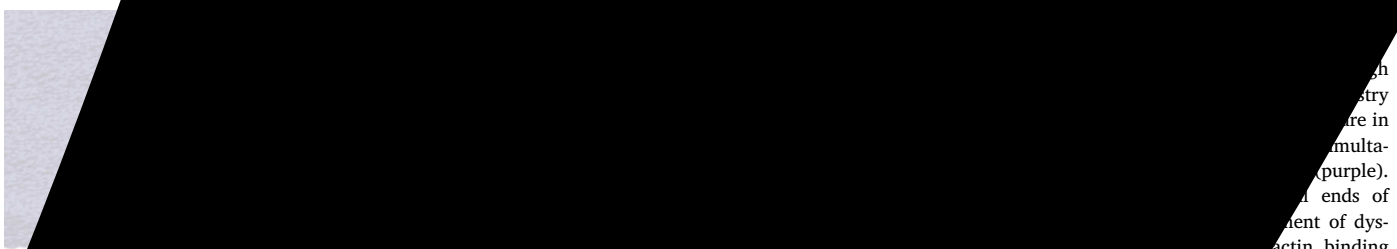

h
try
re in
multa-
purple).
ends of
ient of dys-
actin binding
esult in the re-
ase of interaction

interacti
lized by hydrophob
experimental mapping results as t
group on the UV-photoactivable lipids is at the
phatic chain. Indeed, the pacFA is a long-cha
should be buried in the bilayer part of the bic
aliphatic chain carrying the clickable chemical
accessible to a protein on the outer toroidal surf
to packing defects. However, the specific be
wards anionic bicelles but not towards zwit
that electrostatics or hydrogen bonding could
the recruitment or in the stabilization of d
teractions.

One major conclusion from our work is
does not overlap with the actin binding
simultaneous interaction with these tw
consistent with our previous work bas
assay of ABD2 bound to lipid vesicles
tegrative structural model that we pro
perimental restraints related to the st
domain (DYS R4-19) and the ABD2
and lipids. The binding of ABD2 t
mentation assays has a Kd of ~9
reported previously (Amann et al.
thermophoresis, we measured a s
tion of the same ABD2 fragmen
observations could be of a gre
context.

4.3. Dystrophin actin-binding d
actin-lipid complex

The location of the R11
the middle of the dystroph
tether, keeping the dystr
sarcolemmal cytoskelet
achieved by the widely
dystroglycan anchorin
is supported by the fa
restore part of the
models (Ramos et
central domain. In
teins. In addition
lacking large par
2015). Dystroph
could help to k
length of the
believed to a
some loss of
hypothesis
people, a
between
seems
end c
tethe
esta
the
r

s://

the dystrophin
ol. Chem. 273,

the rod domain actin
80.
py for Duchenne mus-

anks, G.B., Gardner, M.K.,
istinguishes dystrophin from
8.
hin and an integral membrane

Carapito,
Gonzalez de
Cianferani, S., Burlet-Sch
2015. Computational and mass-spectro
validation of missing human proteins: application to
Proteome Res. 14 (9), 3621–3634.
Chen, Y.J., Spence, H.J., Cameron, J.M., Jess, T., Ilsley, J.L.,
interaction of beta-dystroglycan with F-actin. Biochem.
Delalande, O., Molza, A.-E., Dos Santos Morais, R., Chéron,
C., Tascon, C., Giudice, E., Guilbaud, M., Nicolas, A., et
domain forms a complex filament that becomes disorga
Biol. Chem. 293 (18), 6637–6646.
DeWolf, C., McCauley, P., Sikorski, A.F., Winlove, C.P.,
J.C., Gratzer, W.B., 1997. Interaction of dystrophin
branes. Biophys. J. 72, 2599–2604.
Dos Santos Morais, R., Delalande, O., Pérez, J., Moure
Appavou, M.-S., Le Rumeur, E., Hubert, J.-F., Cor
isotropic bicelles: a versatile tool to specifically
ipheral membrane proteins using SANS. Langmu
Dos Santos Morais, R., Delalande, O., Pérez, J., Mias
A., Molza, A.-E., Chéron, A., Raguénès-Nicol,
M.-S., Le Rumeur, E., Combet, S., Hubert, J.-F
changes upon binding to anionic membrane
Duan, D., 2018. Systemic AAV micro-dystrophin
dystrophy. Mol. Ther. 26 (10), 2337–2356.
Ervasti, J.M., Campbell, K.P., 1991. Membrane
protein complex. Cell 66 (6), 1121–1131.
Fiehn, W., Peter, J., Mead, J.F., Gan-Elepano,
lemma, sarcoplasmic reticulum, and mit
Chem. 246, 5617–5620.
Franke, D., Petoukhov, M.V., Konarev, P.V.,
H.D.T., Kikhney, A.G., Hajizadeh, N.R.
ATSAS 2.8: a comprehensive data ana
macromolecular solutions. J. Appl. C
Haberkant, P., Holthuis, J.C.M., 2014. Fa
Biochim. Biophys. Acta Mol. Cell.
Henderson, D.M., Lee, A., Ervasti, J.M.
actin binding domain 1 of dystrop
aggregation. PNAS 107, 9632–96
Henderson, D.M., Lin, A.Y., Thomas,
of dystrophin enhances actin b
Ibraghimov-Beskrovnaya, O., Ervas
Campbell, K.P., 1992. Primar
linking dystrophin to the ext
Jumeau, F., Com, E., Lane, L., Du
Gateau, A., Melaine, N., Gu
Human spermatozoa as a
chromosome-centric hum
Kabsch, W., Sander, C., 198
cognition of hydrogen-
2577–2637.
Kumar, A., Crawford, K.,
S., Duffy, J., Neuma
deficient mice by e
Lai, Y., Thomas, G.D.,
Chamberlain, J.S.
peats 16 and 17
in a mouse mod
Laskowski, R.A., M
program to ch
Appl. Crystal
Lavigne, R., Bec
Direct itera
tein detec
012682.
Le, S., Yu, M
shock
Legarnier,
Rum
rod
Legran
st
M